NANO MICRO small

Supporting Information

for *Small*, DOI: 10.1002/smll.201900379

Strongly Coupled Pyridine-$V_2O_5 \cdot nH_2O$ Nanowires with Intercalation Pseudocapacitance and Stabilized Layer for High Energy Sodium Ion Capacitors

Jun Dong, Yalong Jiang, Qiulong Wei, Shuangshuang Tan, Yanan Xu, Guobin Zhang, Xiaobin Liao, Wei Yang, Qidong Li, Qinyou An, and Liqiang Mai**

Supporting Information

Strongly coupled pyridine-V_2O_5·nH_2O nanowires with intercalation pseudocapacitance and stabilized layer for high energy sodium ion capacitors

*Jun Dong, Yalong Jiang, Qiulong Wei *, Shuangshuang Tan, Yanan Xu, Guobin Zhang, Xiaobin Liao, Wei Yang, Qidong Li, Qinyou An and Liqiang Mai**

J. Dong, Y.L. Jiang, Q.L. Wei, S.S. Tan, Y.N. Xu, G.B. Zhang, X.B. Liao, W. Yang, Q.D. Li, Prof. Q.Y. An, and Prof. L.Q. Mai

State Key Laboratory of Advanced Technology for Materials Synthesis and Processing, International School of Materials Science and Engineering, Wuhan University of Technology, Hubei, Wuhan 430070, P. R. China.

E-mail: mlq518@whut.edu.cn; wql236@163.com

The SI file includes 13 Figures and 4 Tables.

Experimental Section

Synthesis of V_2O_5·nH_2O. The V_2O_5 sol was synthesized by a melt quenching process.[1] In brief, V_2O_5 powder (40 g) melted in air at 800 ^oC for 30 min. Then, the molten liquid was quickly poured into distilled water (2 L) with stirring under water bath (80 ^oC), and then stirring for 24 h at 60 ^oC. The suspensions were obtained. Finally, the suspension was altered for 6 times. A brownish V_2O_5 sol was obtained. The concentration of V_2O_5 sols is 0.048 mol L^{-1}.

Synthesis of pyridine-V_2O_5·nH_2O nanowires. Pyridine-V_2O_5·$n$$H_2O$ nanowires were synthesized by a hydrothermal method. The V_2O_5 sol (62.5 mL) was added into H_2O_2 (5 mL) with stirring for 1h. Then, pyridine (1 mL) was added. The mixed solution was transferred to a Teflon-lined stainless-steel autoclave and heated in an electric oven at 200 ^oC for 4 days. The obtained material was then filtered, washed with deionized water and alcohol, and dried at 70 ^oC for 12 h.

Materials characterization. X-ray diffraction (XRD) measurements were conducted by using a D8 Advance X-ray diffractometer with a non-monochromated Cu Kα X-ray source at room temperature. Scanning electron microscopy (SEM) images were collected by using a JEOL-7100F microscope. Transmission electron microscopy and high-resolution TEM (HRTEM) images were collected by

using a JEM-2100F STEM/EDS microscope. Thermogravimetric (TG) analysis was performed using NETZSCH-STA449F5 thermoanalyzer. CHN elemental analysis was performed by Vario EL cube instrument. Fourier transform infrared (FT-IR) transmittance spectra were recorded using the 60-SXB IR spectrometer. The transmission mode is chosen in the IR spectrometry. X-ray photoelectron spectroscopy (XPS) was recorded with a VG Multilab 2000. The electronical conductivity was measured by the probe station and semiconductor device analyzer (B1500A).

Electrochemical measurements. The electrochemical properties were investigated by assembly of 2016 coin cells in an Ar-filled glove box. The working electrode materials were prepared by mixing 70% active material, 20% conductive carbon and 10% carboxyl methyl cellulose (CMC). Then the mixed slurry was cast onto carbon coated Al foil and dried in a vacuum oven at 70 ^{o}C for 12 h. The mass loading of active materials was 2 mg cm^{-2}. The graphitic mesocarbon microbead (MCMB) anode (HF-Kejing Co., Ltd) were prepared by mixing 92% active material and 8% CMC binder, and then coated on a carbon coated Al foil. After drying in vacuum oven at 120 °C for 12 hours. Active material (25 mg) and multi-walled carbon nanotubes (MWCNT, HF-Kejing Co., Ltd) (5 mg) were mixed with alcohol, and then a film was prepared by suction filtrating for *ex*-FTIR test. At half-cell tests, sodium bulks (China Energy Lithium Co., Ltd.) were cut into small pieces and used as the counter electrode. Glass fiber separator was used. The electrolyte was composed of 1 M $NaPF_6$ in diglyme. For assembling the full pyridine-$V_2O_5{\cdot}nH_2O$//MCMB sodium ion capacitor, pre-sodiated MCMB at 0.02 V were prepared to provide the shuttle of Na^+ ions in between the cathode and anode. The mass ratio of pyridine-$V_2O_5{\cdot}nH_2O$ to MCMB was fixed at 1:1.5 according the stored charges balance in between cathode and anode ($C^+ \times m^+ = C^- \times m^-$). Galvanostatic charge/discharge and cyclic voltammetry (CV) were tested using Bio-Logic VMP3 electrochemical workstation. All the measurements were carried out at room temperature.

Density functional theory (DFT) calculations.

The present calculations were carried out by using the projector augmented wave (PAW)[2] method within the DFT as implemented in the Vienna ab initio simulation package (VASP).[3] The generalized

gradient approximation (GGA) in the forms of Perdew-Burke-Ernzerhof (PBE)[4] is used to treat the exchange-correlation energy. When the cutoff energy increases to 500 eV, the energy of pyridine-$V_2O_5{\cdot}nH_2O$ system remains nearly unchanged. Thus, the energy cutoff of 500 eV was chosen for wave functions expanded in plane wave basis (Figure S13). All atoms are allowed to be relaxed until forces are less than 0.01 eV $Å^{-1}$. For the Brillouin-zone sampling, 4×4×4 of k-point were set for the structure relaxation and increased to 10 × 10 × 10 for the electronic structure calculations. Ultrasoft pseudopotentials were used to describe the interaction of ionic core and valence electrons.

Calculation of the chemical formulas of pyridine-$V_2O_5{\cdot}nH_2O$ and $V_2O_5{\cdot}nH_2O$

The chemical formulas of pyridine-$V_2O_5{\cdot}nH_2O$ and $V_2O_5{\cdot}nH_2O$ are denoted as $V_2O_5{\cdot}yH_2O$ and $V_2O_5{\cdot}yH_2O{\cdot}xC_5H_5N$ for detailed calculation.

The molecular weight is shown as follows:

$M_{V_2O_5} = 181.88\ g\ mol^{-1},\ M_{C_5H_5N} = 79.1\ g\ mol^{-1}, M_{H_2O} = 18\ g\ mol^{-1}, M_N = 14\ g\ mol^{-1}.$

The CHN analysis shows the nitrogen mass content (N wt.%) of xC_5H_5N-$V_2O_5{\cdot}yH_2O$ is = 3.18 wt.%. Through TG test, the weight loss should include the content of pyridine and H_2O. The total mass loss (Total wt.%) of pyridine-$V_2O_5{\cdot}nH_2O$ and $V_2O_5{\cdot}nH_2O$ is respectively 30.51% and 7.3%. The chemical formulas can be calculated by following Equation S1 and S2:

$$xM_N = \left(M_{V_2O_5} + xM_{C_5H_5N} + yM_{H_2O}\right) \times \text{N}\ wt.\% \qquad \text{(S1)}$$

$$xM_{C_5H_5N} + yM_{H_2O} = \left(M_{V_2O_5} + xM_{C_5H_5N} + yM_{H_2O}\right) \times \text{T}\ wt.\% \qquad \text{(S2)}$$

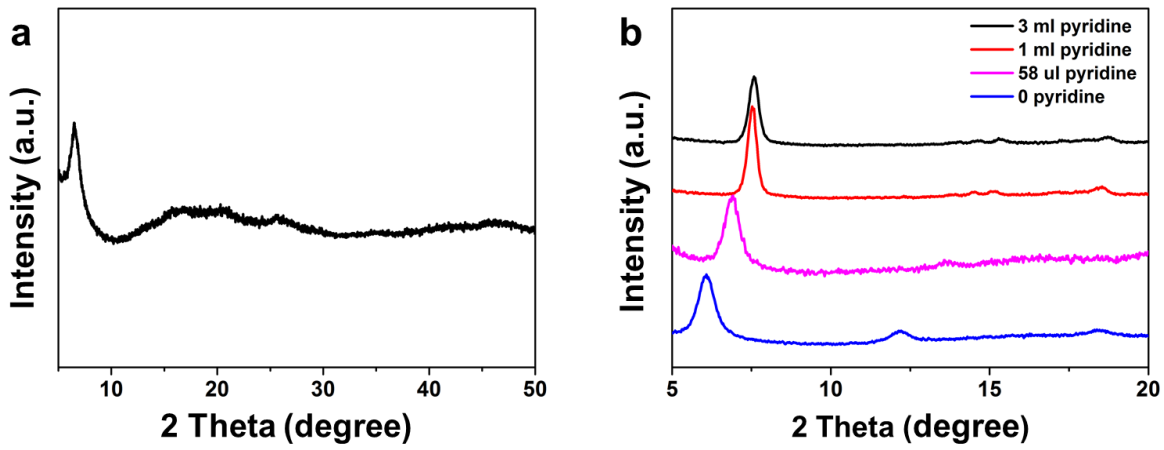

Figure S1. (a, b) XRD patterns of $V_2O_5 \cdot nH_2O$ and samples synthesized by different addition amount of pyridine, respectively.

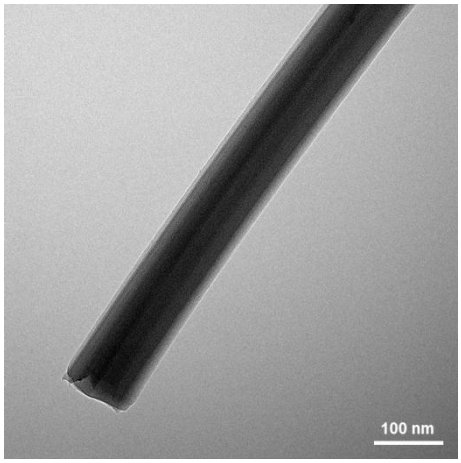

Figure S2. TEM images of pyridine-$V_2O_5 \cdot nH_2O$

Table S1.CHN chemical compositions and thermogravimetric analysis data in the range of 100-700 °C.

Sample	Addition amount of Pyridine	N(mass %)	C(mass %)	C/N moar ratio	TG (mass loss %)
Pyridine - $V_2O_5{\cdot}nH_2O$	0 µl	0	0	0	—
	58 µl	0.135	0.683	5.06	—
	1 ml	0.227	1.139	5.02	30.51
	3 ml	0.225	1.113	4.95	—
$V_2O_5{\cdot}nH_2O$	—	0	0	0	7.3

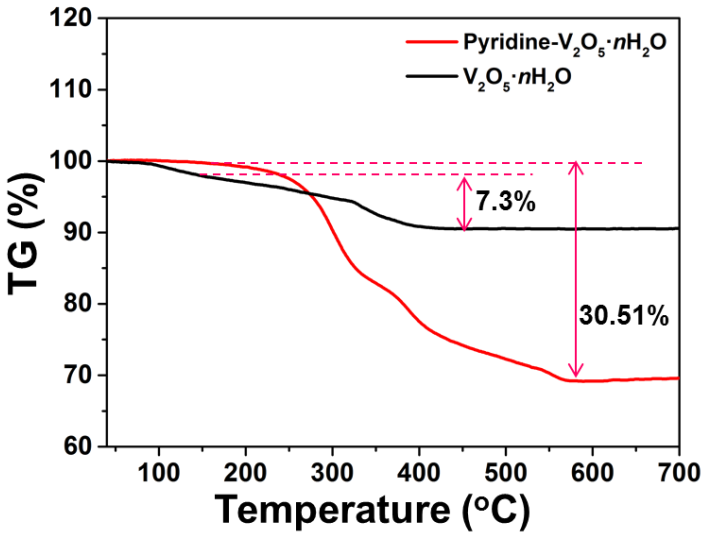

Figure S3. TG curves of pyridine-$V_2O_5{\cdot}nH_2O$ and $V_2O_5{\cdot}nH_2O$.

Table S2. Frequencies and assignment of the FTIR absorption bands of pyridine-$V_2O_5{\cdot}nH_2O$ and $V_2O_5{\cdot}nH_2O$, respectively.

FTIR absorption bands	Assignment	
	pyridine-$V_2O_5{\cdot}nH_2O$	$V_2O_5{\cdot}nH_2O$
3411	*v* (O-H)	*v* (O-H)
3230(v_{7a})		—
3164	*v* (N-H)	—
3128		—
3086		—
3064 (v_{12})	*v* (C-H)	—
1633 (v_{8a})	*v* (C-C)	—
1617 (v_{8b})	*v* (O-H)	*v* (O-H)
1537 (v_{19b})	*v* (C-C)	—
1482 (v_{19a})	*v* (C-C)	—
1332 (v_3)	*δ* (C-H)	—
1251 (δ_{9b})	*δ* (N-H)	—
1012	—	*v* (V=O)
1002	*v* (V^{5+}=O)	—
966	*v* (V^{4+}=O)	—
756	*δ* (V-O-V)	*δ* (V-O-V)
677 (v_{11})	*v* (C-H)	—
515	*δ* (V-O)	*δ* (V-O)

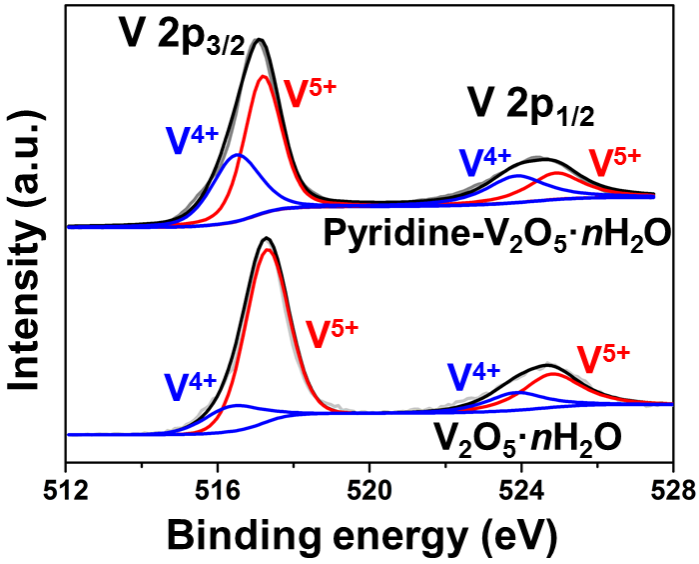

Figure S4. V 2p XPS spectra of pyridine-$V_2O_5{\cdot}nH_2O$ and $V_2O_5{\cdot}nH_2O$, respectively.

Table S3. The percentage of V^{4+}/V^{5+} in $V_2O_5{\cdot}nH_2O$ and pyridine-$V_2O_5{\cdot}nH_2O$ according to the XPS analysis.

Sample	V^{4+}/V^{5+}
$V_2O_5{\cdot}nH_2O$	18.7%
Pyridine-$V_2O_5{\cdot}nH_2O$	42.6%

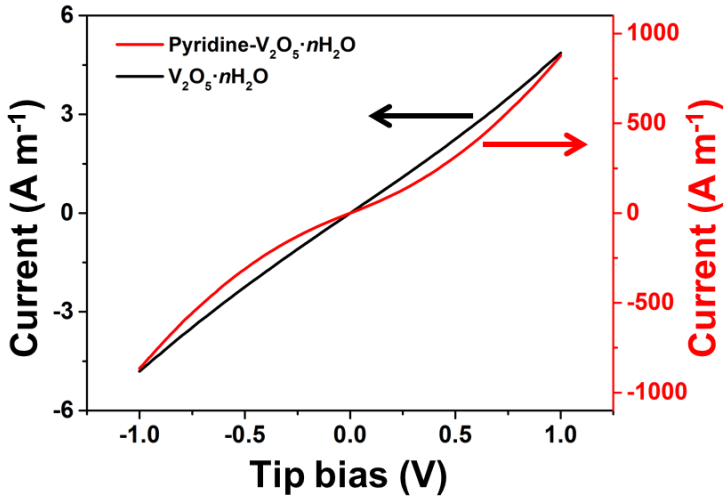

Figure S5. *I-V* curves of pyridine-$V_2O_5{\cdot}nH_2O$ and $V_2O_5{\cdot}nH_2O$, respectively.

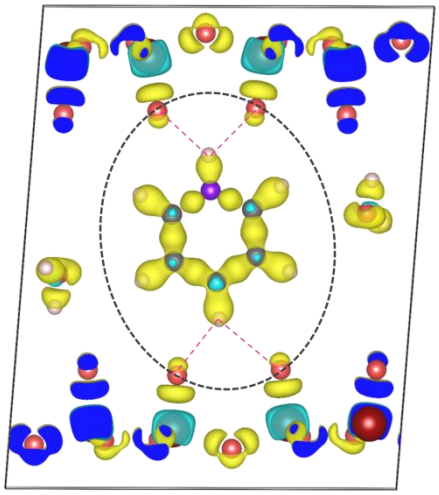

Figure S6. Charge-density difference of pyridine-$V_2O_5{\cdot}nH_2O$

Table S4. A comparison for the experimental conditions and cycle capabilities of vanadium oxides-based cathodes reported in literatures.

Cathode mateirals	Potencial window [V vs. Na^+/Na]	Active material: conductive additivity: binder	Cycling capability	Mass loading [mg cm^{-2}]	Ref.
Bilayered V_2O_5	1-4	70:20:10	100 cycles, 117 mAh g^{-1} (640 mA g^{-1})	—	6
$V_2O_5 \cdot nH_2O$	1-4	70:20:10	30 cycles, 180 mAh g^{-1} (100 mA g^{-1})	2-3	1
OrthorhombicV_2O_5	1-4	70:20:10	100 cycles, 142mAh g^{-1} (20 mA g^{-1})	—	7
Nanocrystalline V_2O_5	1.5-3.8	80:10:10	500 cycles, 176 mAh g^{-1} (10 mA g^{-1})	—	8
Fe-VO_x	1-4	70:20:10	50 cycles, 148mAh g^{-1} (100 mA g^{-1})	2-3	5
Orthorhombic V_2O_5	1.5-3.8	70:20:10	20 cycles, 178 mAh g^{-1} (40 mA g^{-1})	1-1.3	9
V_2O_5 aerogel	1.5-4	70:20:10	—	—	10
Pyridine-$V_2O_5 \cdot nH_2O$	1-4	70:20:10	1000 cycles, 86 mAh g^{-1} (1000mA g^{-1})	2	This work

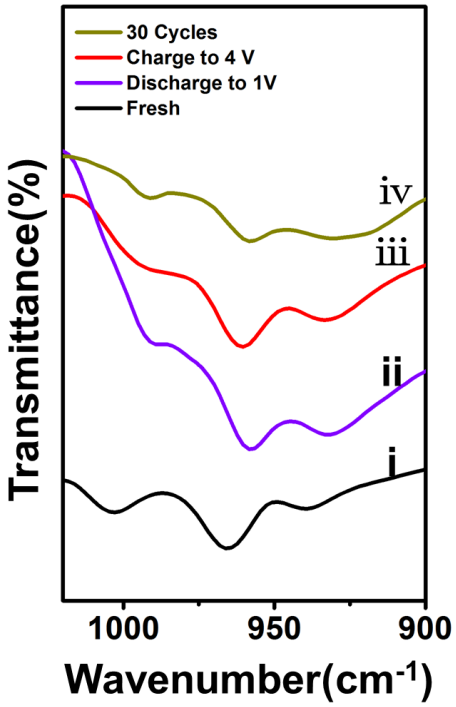

Figure S7. *Ex*-FTIR spectra of pyridine-$V_2O_5 \cdot nH_2O$ cathode at the wavenumber from 1020 to 900 cm^{-1} at different charge-discharge states.

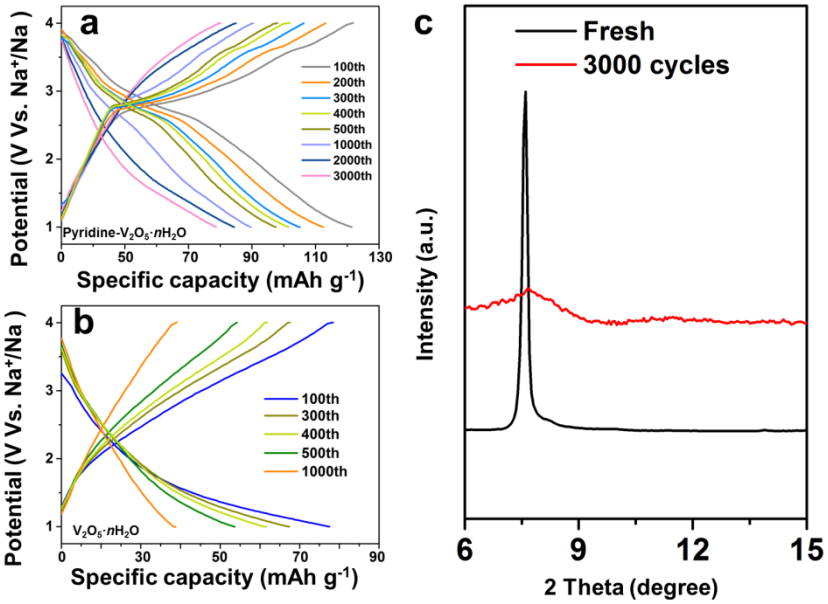

Figure S8. (a, b) Charge-discharge curves of pyridine-$V_2O_5 \cdot nH_2O$ and $V_2O_5 \cdot nH_2O$ after different cycles at 1 A g^{-1}. (b) *Ex-situ* XRD patterns at the fresh state and after 3000 cycles.

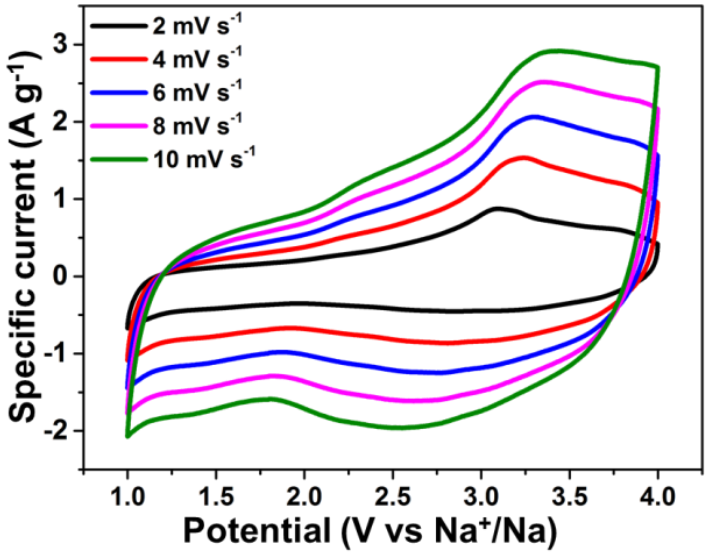

Figure S9. CV curves of pyridine-$V_2O_5 \cdot nH_2O$ at various scan rates from 2 to 10 mV s^{-1}.

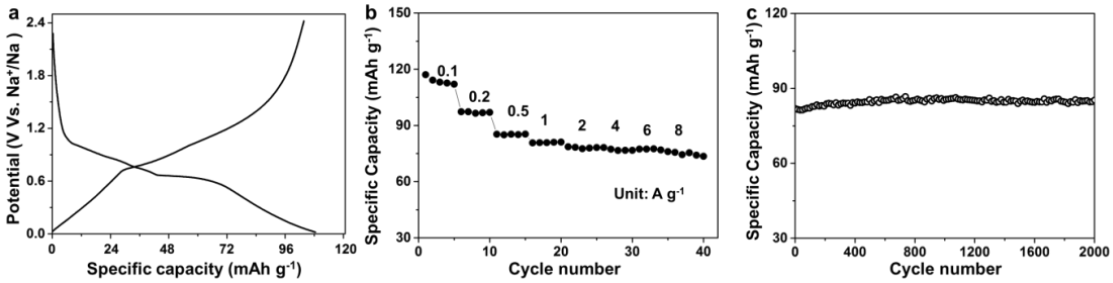

Figure S10. The electrochemical performance of MCMB anode. Charge–discharge curves at 0.1 A g^{-1} (a), rate performance (b) and cycling performance at 1 A g^{-1} (c).

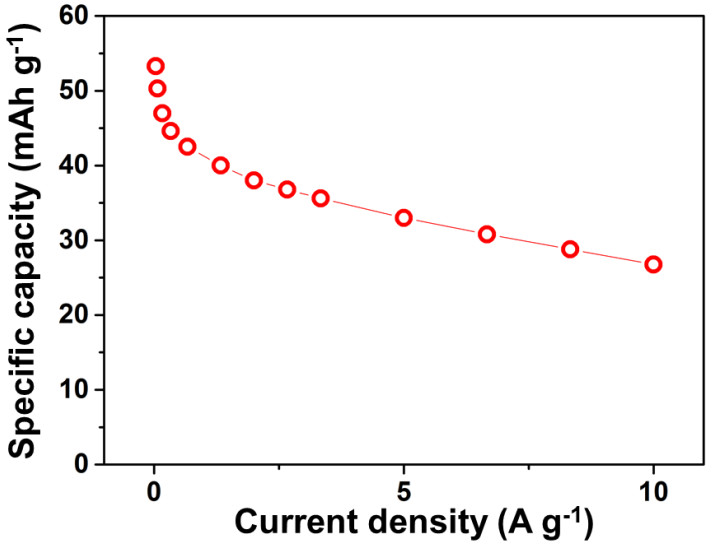

Figure S11. The rate performance of pyridine-$V_2O_5 \cdot nH_2O$//MCMB SIC.

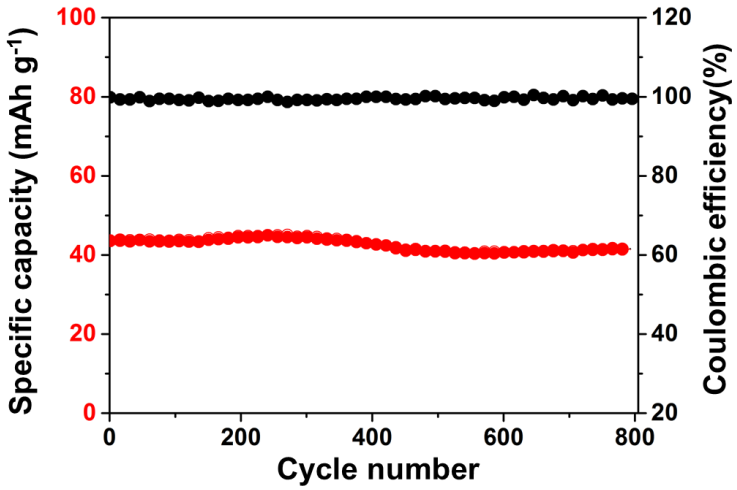

Figure S12. The cycling performance of pyridine-$V_2O_5{\cdot}nH_2O$//MCMB SIC.

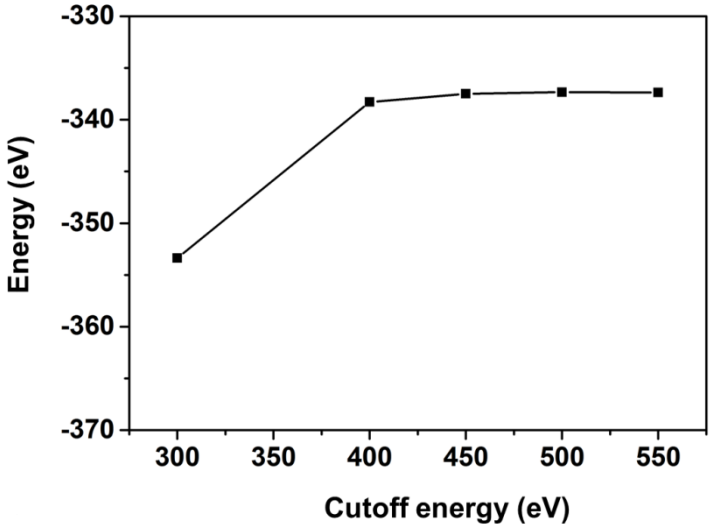

Figure S13. The test of cutoff energy for pyridine-$V_2O_5{\cdot}nH_2O$.

REFERENCES

1. Q. Wei, J. Liu, W. Feng, J. Sheng, X. Tian, L. He, Q. An, L. Mai, *J. Mater. Chem. A* **2015**, *3*, 8070.
2. G. Kresse and D. *Joubert, Phys. Rev. B* **1999,** 59, 1758–1775.
3. G. Kresse and J. Furthmüller, *Comput. Mater. Sci.* **1996,** 6, 15–50.
4. J. P. Perdew, K. Burke and M. Ernzerhof, *Phys. Rev. L* **1998,** 77, 3865–3868.
5. Q. Wei, Z. Jiang, S. Tan, Q. Li, L. Huang, M. Yan, L. Zhou, Q. An, L. Mai, *ACS Appl. Mater. Inter.* **2015**, *7*, 18211.6. Su, D.; Wang, G. *ACS Nano* **2013,** 7, 11218-11226.
6. D. Su, G. Wang, *ACS Nano* **2013**, *7*, 11218.
7. D. W. Su, S. X. Dou, G. X. Wang, *J. Mater. Chem. A* **2014**, *2*, 11185.
8. H. Y. Li, C. H. Yang, C. M. Tseng, S. W. Lee, C. C. Yang, T. Y. Wu, J. K. Chang, *J. Power Sources* **2015**, *285*, 418.
9. V. Raju, J. Rains, C. Gates, W. Luo, X. Wang, W. F. Stickle, G. D. Stucky, X. Ji, *Nano Lett.* **2014**, *14*, 4119.
10. A. Moretti, F. Maroni, I. Osada, F. Nobili, S. Passerini, *Chemelectrochem* **2015**, *2*, 529.